SPECTRAL AMPLITUDE AND PHASE CHARACTERISTICS OF SHALLOW CRUSTAL EARTHQUAKE BASED ON LINEAR INVERSION OF GROUND MOTION SPECTRA AND SOME ENGINEERING APPLICATIONS

T. Itoi[1], I. Nagashima[1] and Y. Uchiyama[1]

[1] *Research Engineer, Technology Center, Taisei Corporation, Yokohama Japan*
Email: ititty00@pub.taisei.co.jp

ABSTRACT:

An inversion method is applied to crustal earthquakes in Japan. Qs value for propagation path is evaluated from spectral amplitudes, and the scattering due to propagation path is evaluated from group delay times. Using the results, an envelope model for stochastic Green's function on rock sites is proposed. Ground motion simulation is also conducted considering site effects using a transfer function between neighboring stations.

KEYWORDS: 2007 Noto Hanto Earthquake, Site effect, Propagation path effect, Crustal Earthquake, Linear inversion

1. INTRODUCTION

For precise simulation of earthquake ground motions, the effects of source, propagation path and local site should be considered. For that purpose, this study performs spectral studies on observed ground motions for shallow crustal earthquakes in Japan.
A conventional inversion method (Andrews, 1981; Iwata & Irikura, 1986) is widely applied to evaluate these effects in spectral amplitudes. Similarly, propagation path and local sediment affect the scattering of earthquake ground motions. The heterogeneity of medium properties is considered one of the reasons. These effects should be considered in ground motion simulation. Generally, the local site effects, such as basin effects, are considered dominant (e.g. Birgoren & Irilura, 2005). The effects of propagation path on the scattering, however, cannot be negligible for ground motion simulation especially on rock sites (e.g. Sawada 1998; Sato 2004). Therefore, these effects should be evaluated, independent from local site effects. For that purpose, an inversion method is applied to the spectral phases, i.e. group delay times, as well as the spectral amplitudes.
Then, two applications are carried out using the results obtained, considering the propagation path effect as well as the site amplification effect. Firstly, a stochastic envelope model is proposed for a stochastic Green's function (Boore 1983; Kamae et al., 1991) on rock sites, which simulates the high frequency spectral phase stochastically. The second application is a simulation of ground motions using an empirical transfer functions between neighboring stations, considering local site effects.

2. PROPAGATION AND SITE CHARACTERISTICS BASED ON LINEAR INVERSION

2.1 Dataset

As shown in Figure 2.1 and Table 2.1, we analyzed ground motion records of 17 crustal earthquakes (M3.9 ~ 5.2) at Noto region in Japan from 2002 to 2007, most of which were the aftershock records of the 2007 Noto Hanto (Mw 6.9) Earthquakes. 37 stations including borehole stations were selected as shown in Figure 2.1. The hypocenter distances are restricted from 10 km to 100 km.
For each horizontal component, S wave beginning times were detected visually and the duration time of the time window for S wave selection was fixed to 60 seconds, where the time window was tapered both at the beginning and the end. Then, spectral amplitudes for S waves (0.5~15Hz) were calculated for each horizontal component, which were smoothed using the Parzen window (0.3 Hz) and sum of squares for two horizontal components were calculated.

Similarly, group delay times for S waves were calculated for each horizontal component. Then, average of group delay times (e.g. Izumi & Katsukura, 1983) were calculated for 1/1 octave band filter (center frequency f_0= 1, 2, 4 and 8 Hz) in the frequency range as follows:

$$\mu_{tgr}(f_0) = \frac{1}{S}\int_{f_L}^{f_H} A(f)^2 \cdot t_{gr}(f)\,df \tag{2.1}$$

where,

$$f_L = f_0/\sqrt{2},\ f_H = \sqrt{2}\,f_0 \tag{2.2}$$

$$S = \int_{f_L}^{f_H} A(f)^2\,df \tag{2.3}$$

Similarly, variance of group delay times were calculated as follows:

$$\sigma_{tgr}{}^2(f_0) = \frac{1}{S}\int_{f_L}^{f_H} A(f)^2 \cdot \left(t_{gr}(f) - \mu_{tgr}(f_0)\right)^2 df \tag{2.4}$$

They were calculated for each horizontal component and averaged for two components.

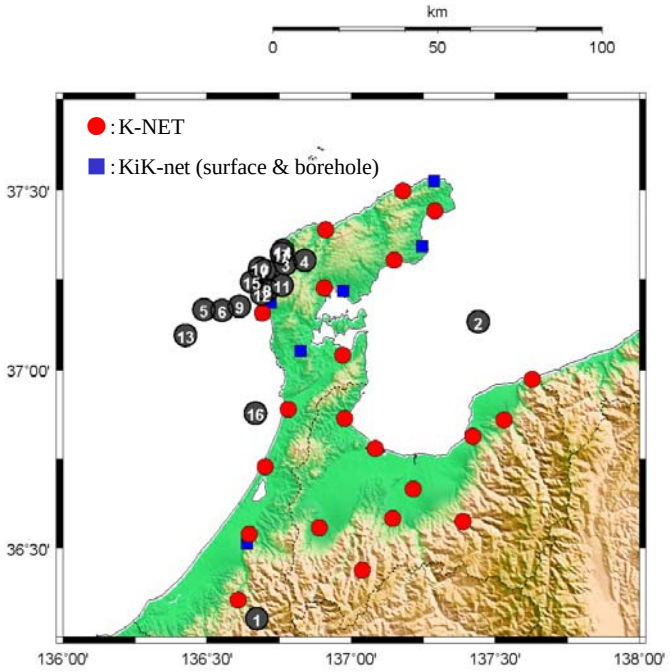

Figure 2.1 Epicenter for earthquakes and location of stations

Table 2.1 List of earthquakes (from JMA)

	Date	Time	M_J
①	2002/11/17	13:47:54.0	4.7
②	2006/5/4	10:17:29.2	3.9
③	2007/3/25	15:43:30.6	4.0
④	2007/3/25	18:11:45.2	5.2
⑤	2007/3/26	7:16:36.5	5.0
⑥	2007/3/26	14:46:34.7	4.5
⑦	2007/3/26	18:02:52.5	4.2
⑧	2007/3/28	8:08:14.6	4.6
⑨	2007/3/28	10:51:02.6	4.0
⑩	2007/3/28	13:05:31.1	4.7
⑪	2007/3/31	8:09:46.9	4.4
⑫	2007/4/2	2:51:44.4	4.0
⑬	2007/4/6	2:17:30.8	4.7
⑭	2007/5/2	20:44:38.2	4.7
⑮	2007/6/11	3:45:13.9	5.0
⑯	2007/6/22	3:34:14.4	4.6
⑰	2007/7/9	16:00:34.3	4.2

2.2 Linear Inversion Method

The observed quantity, e.g. spectral amplitude, o_{ij} from *i*-th event recorded at *j*-th station is assumed to be decomposed to the source, propagation path and site effects as follows:

$$o_{ij} = s_i + p_{ij} + g_j \tag{2.5}$$

where s_i, p_{ij} and g_j are the source, propagation path and site effects respectively. p_{ij} is assumed to depend on the hypocenter distance as follows:

$$p_{ij} = \alpha \cdot r_{ij}{}^k \tag{2.6}$$

where α, k and r_{ij} are the constant, the power index and the hypocenter distance from *i*-th event at *j*-th station respectively.

In matrix form, Eqns. (2.5) and (2.6) are expressed as follows:

$$\begin{bmatrix} o_{11} \\ \vdots \\ o_{1n} \\ o_{21} \\ \vdots \\ o_{2n} \\ \vdots \\ o_{m1} \\ \vdots \\ o_{mn} \end{bmatrix} = \begin{bmatrix} 1 & 0 & \cdots & 0 & 1 & 0 & 0 & r_{11}^{\ k} \\ \vdots & \vdots & \vdots & \vdots & 0 & \ddots & 0 & \vdots \\ 1 & 0 & 0 & 0 & 0 & 0 & 1 & r_{1n}^{\ k} \\ 0 & 1 & 0 & 0 & 1 & 0 & 0 & r_{21}^{\ k} \\ \vdots & \vdots & \vdots & \vdots & 0 & \ddots & 0 & \vdots \\ 0 & 1 & 0 & 0 & 0 & 0 & 1 & r_{2n}^{\ k} \\ \vdots & \vdots & \vdots & \vdots & \vdots & \vdots & \vdots & \vdots \\ 0 & 0 & 0 & 1 & 1 & 0 & 0 & r_{m1}^{\ k} \\ \vdots & \vdots & \vdots & \vdots & 0 & \ddots & 0 & \vdots \\ 0 & 0 & 0 & 1 & 0 & 0 & 1 & r_{mn}^{\ k} \end{bmatrix} \begin{bmatrix} s_1 \\ \vdots \\ s_m \\ g_1 \\ \vdots \\ g_n \\ \alpha \end{bmatrix} \tag{2.7}$$

If the observed quantities are expressed as the summation of the source, propagation path and site effects as a linear equation in Eqn. (2.7), these effects are separately estimated by solving the equation using the singular value decomposition technique. In this study, an inversion method outlined above is applied to S wave beginning times, spectral amplitudes, average and variance of group delay times.

S wave beginning times from *i*-th event recorded at *j*-th station ${}_{o}t_{ij}$ are expressed as follows:

$$ {}_{o}t_{ij} = {}_{s}t_{i} + {}_{p}t_{ij} + {}_{g}t_{j} \tag{2.8}$$

where ${}_{s}t_{i}$, ${}_{p}t_{ij}$ and ${}_{g}t_{j}$ are the source, propagation path and site term respectively. The propagation path term ${}_{p}t_{ij}$ is expressed as follows:

$$ {}_{p}t_{ij} = r_{ij} / \beta \tag{2.9}$$

where β is S wave velocity, which is evaluated from an inversion analysis. If $t = 0$ is given by the earthquake origin times, the source terms are expected to have zero value on average.

The spectral amplitudes from *i*-th event recorded at *j*-th station are expressed as follows:

$$ {}_{o}A_{ij}(f) = {}_{s}A_{i}(f) \cdot \left(r_{ij}^{-1} \cdot {}_{p}A_{ij}(f) \right) \cdot {}_{g}A_{j}(f) \tag{2.10}$$

$$ \log\left({}_{o}A_{ij}(f) \cdot r_{ij} \right) = \log\left({}_{s}A_{i}(f) \right) + \log\left({}_{p}A_{ij}(f) \right) + \log\left({}_{g}A_{j}(f) \right) \tag{2.11}$$

where ${}_{s}A_{i}$, ${}_{p}A_{ij}$ and ${}_{g}A_{j}$ are the source, propagation path and site factors. The propagation path factor ${}_{p}A_{ij}$ is expressed as follows:

$$ {}_{p}A_{ij}(f) = e^{-\pi f \cdot r_{ij} / Q(f) \beta} \quad \therefore \log\left({}_{p}A_{ij}(f) \right) = -\pi f \cdot r_{ij} / Q(f) \beta \tag{2.12}$$

The spectral phase characteristics, i.e. average and variance of observed group delay time ${}_{o}\mu_{tgr}$ and ${}_{o}\sigma_{tgr}$, are expressed as sum of the source, propagation path and site terms as follows:

$$ {}_{o}\mu_{tgr,ij}(f) = {}_{s}\mu_{tgr,i}(f) + {}_{p}\mu_{tgr,ij}(f) + {}_{g}\mu_{tgr,j}(f) \tag{2.13}$$

$$ {}_{o}\sigma_{tgr,ij}^{\ 2}(f) = {}_{s}\sigma_{tgr,i}^{\ 2}(f) + {}_{p}\sigma_{tgr,ij}^{\ 2}(f) + {}_{g}\sigma_{tgr,j}^{\ 2}(f) \tag{2.14}$$

where, the propagation path term ${}_{p}\mu_{tgr,ij}$ and ${}_{p}\sigma_{tgr,ij}$, is assumed to depend on the hypocenter distance as follows:

$$ {}_{p}\mu_{tgr,ij}(f) = a \cdot r_{ij}^{\ m} \tag{2.15}$$

$$ {}_{p}\sigma_{tgr,ij}(f) = b \cdot r_{ij}^{\ n} \tag{2.16}$$

The power index *m* and *n* need to be fixed prior to an inversion analysis, which is discussed in 2.3.3.

2.3 Results

2.3.1 S wave beginning time

Figure 2.2 shows the site terms for S wave beginning times at each station under the condition that the site term at TYM011 was assumed to zero. At stations on deep sediments (e.g. TYM005), the site terms were larger than rock stations (e.g. TYM011) due to their low S wave velocities of sedimentary layers. S wave velocity β for propagation path was evaluated 3.44 km/s, which was used in the analysis for the spectral amplitudes hereafter.

2.3.2 Spectral amplitude

Figure 2.3 shows Qs value estimated by an inversion analysis of the spectral amplitudes. The least square regression method gave $Qs = 29.0f^{1.24}$. Figure 2.4 compares the Qs value to those of crustal earthquakes in other regions (e.g. Sato, 2006). Our result was comparable to those of crustal earthquakes at other regions in Japan.

2.3.3 Group delay time

Figure 2.5 and Figure 2.6 shows average and standard deviation of group delay times calculated for all stations for all earthquakes. In Figures, the slope and vertical intercept represent the scattering characteristics of propagation path, while the scatterings along the vertical axis represent the difference in the effects between local sites and earthquakes. In this study, dependence of group delay times on the hypocenter distance was assumed as follows:

$$\mu_{tgr}(f) = a \cdot \min(r, 70) \tag{2.17}$$

$$\sigma_{tgr}(f) = b \cdot \min(r^{0.5}, 70^{0.5}) \tag{2.18}$$

Figure 2.7 and Figure 2.8 shows the constants *a* and *b* evaluated by an inversion analysis. Both *a* and *b* slightly decreased as frequency increases.

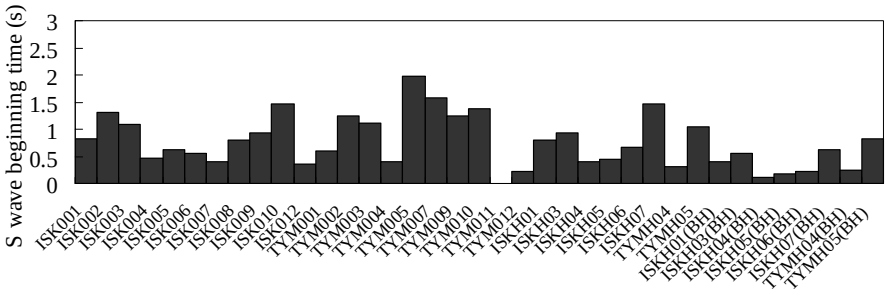

Figure 2.2 Site term for S wave beginning time

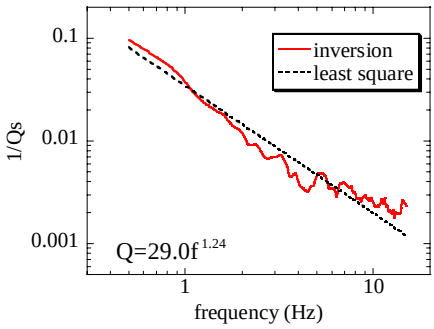

Figure 2.3 Qs value estimated by inversion method

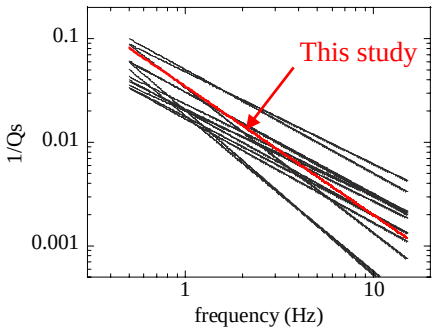

Figure 2.4 Comparison of Qs for crustal earthquakes in Japan

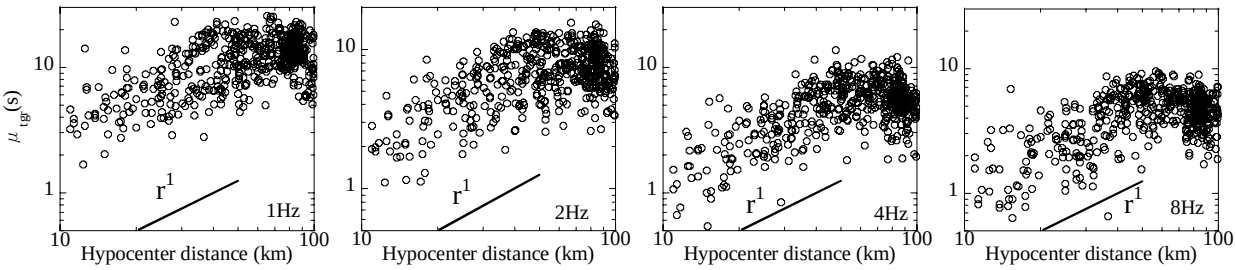

Figure 2.5 Dependence of μ_{tgr} on hypocenter distances for all earthquakes (1~8Hz)

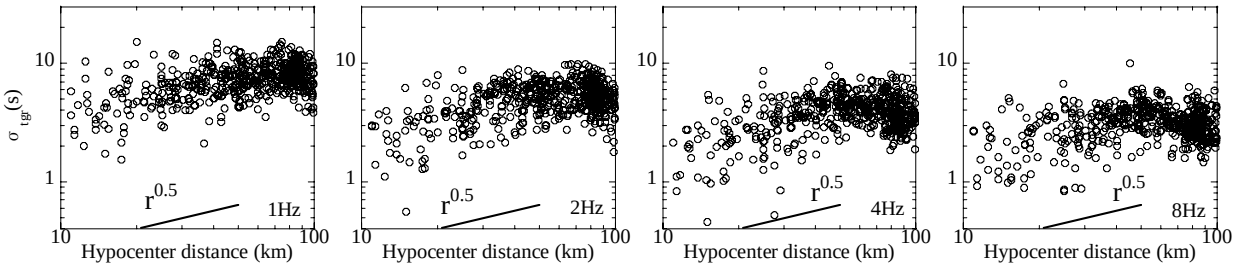

Figure 2.6 Dependence of σ_{tgr} on hypocenter distances for all earthquakes (1~8Hz)

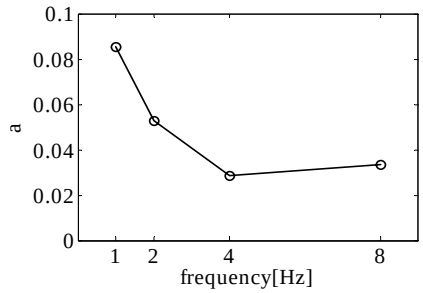

Figure 2.7 Constant *a* evaluated from inversion analysis of μ_{tgr} (1~8Hz)

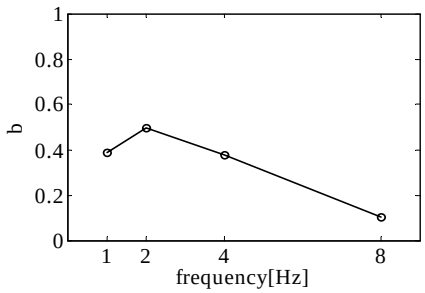

Figure 2.8 Constant *b* evaluated from inversion analysis of σ_{tgr} (1~8Hz)

3. SIMULATION OF EARTHQUAKE GROUND MOTION

3.1 Stochastic Green's Function on Seismic Bedrock

3.1.1 Envelope model for propagation path

A methodology to treat the effects of scattering due to propagation path in ground motion simulation is proposed. For simulation of broadband ground motions using a hybrid simulation technique, Coherence between a deterministic result for lower frequency and a stochastic result for higher frequency is required in intermediate frequency range (0.5 ~ 1Hz). An improved method (Kagawa, 2004) was proposed for that purpose, to generate stochastic Green's functions consistent with seismic source time functions in low frequency range. In the method proposed by Kagawa, however, an envelope shape was determined based on the source characteristics proposed by Boore (1983) and the scattering due to propagation path was not considered. A method proposed in this study can improve this inadequacy considering these effects.

For that purpose, group delay times for a stochastic Green's function are generated as follows; As shown in Figure 3.1, group delay times for lower frequency are fixed deterministically to zero for coherence at the intermediate frequency range as discussed, whereas those for higher frequency were randomly generated. Transient frequency from a deterministic range to a stochastic range was assumed to depend on a travel distance, or a hypocenter distance *r*, similar to a radiation pattern model proposed by Onishi & Horike (2000). In this study, the lognormal distribution was assumed for random numbers. As in Figure 2.5 and Figure 2.6, observed group delay times for low frequency (1, 2 Hz) were larger than those for high frequency, which had adverse tendency with a proposed model in Figure 3.1. One of possible reasons considered were that a proposed model did not consider surface waves but body waves, while observed group delay times for low frequencies were affected by surface waves, which have the dispersion characteristics.

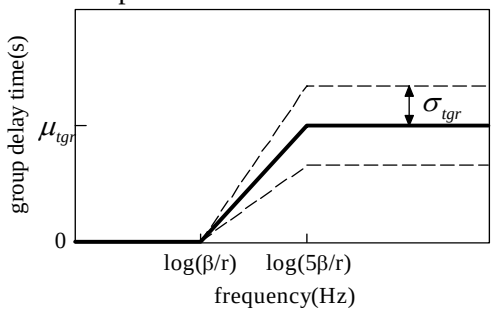

Figure 3.1 Group delay time model for propagation path

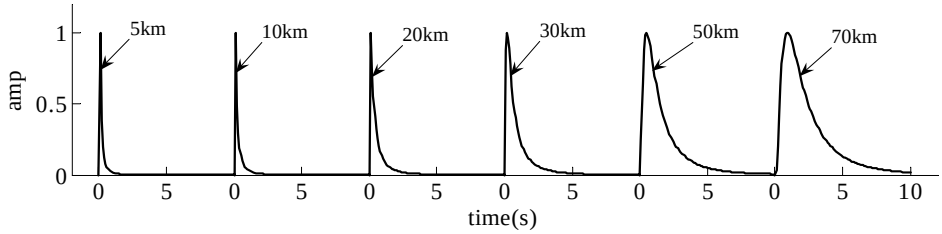

Figure 3.2 Envelope shape proposed for propagation path from inversion results ($f > 5\beta/r$)

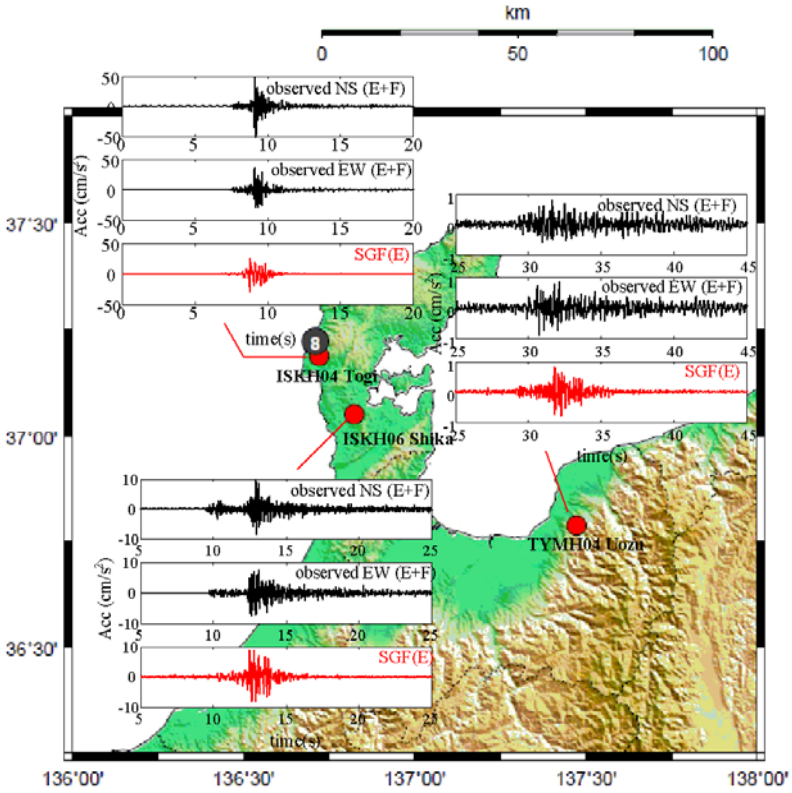

Figure 3.3 Comparison between observed borehole records and simulation results (>3Hz) for M_J 4.6 earthquake at 8:08 Mar 28 2008 (No. 8)

In a simulation, mean values between 2 ~ 8 Hz were used in a simulation for simplification (a = 0.038, b = 0.33), though the constants a and b in Figure 2.7 and Figure 2.8 slightly depended on frequency as shown in Figure 2.7 and Figure 2.8.

Figure 3.2 shows dependence of proposed envelope shapes on a hypocenter distance. Duration of envelope increases as a hypocenter distance increases, to be consistent with observation.

Figure 3.3 shows comparison between acceleration time history (>3Hz) for borehole stations and for simulated stochastic Green's function. The duration for simulated motion was shorter than the observed motions. One of possible reasons is that simulated ground motions were for incident waves (E), while observed ground motions were affected both by incident waves (E), and by reflected waves (F), from sedimentary layer overlying stations as well as surface waves.

3.2 Ground Motion Simulation Using Records at Neighboring Station

A procedure for ground motion simulation is proposed and demonstrated using a transfer function between neighboring stations. When evaluating a transfer function between two stations, the attenuation characteristics should be excluded because the site effects are considered. Based on these requirements, a Fourier amplitude ratio between stations was expressed as follows:

$$R_{i,j\to k}(f) = \frac{A_{ik}(f)}{A_{ij}(f)} \cdot \frac{r_{ik}}{r_{ij}} \cdot e^{\pi f \cdot (r_{ij} - r_{ik}) / Q(f)\beta} \tag{3.1}$$

Then, geometrically averaged for N events as follows:

$$R_{j\to k}(f) = \left(\prod_{i=1}^{N} R_{i,j\to k}(f) \right)^{1/N} \tag{3.2}$$

where, $A_{ij}(f)$ is a Fourier amplitude for i-th event at j-th station, which was calculated for radial and transverse component.

Figure 3.4 shows Fourier amplitude ratios from borehole station at ISKH04 (Togi) to ISK005 (Anamizu). Peaks were observed at 1.3, 3 and 5 Hz both in amplitudes of radial and transverse components.

Then, ground motion for *i*-th event at *k*-th station $x_{ik}(t)$ was simulated from records at neighboring *j*-th station $x_{ij}(t)$ using both results of inversion analyses in Chapter 2 and a Fourier amplitude ratio evaluated from Eqn. (3.2) as follows:

$$F_{ik}(f) = R_{j\to k}(f)\cdot F_{ij}(f)\cdot \frac{r_{ij}}{r_{ik}}\cdot e^{\pi f\cdot (r_{ik}-r_{ij})/Q(f)\beta}\cdot e^{-i2\pi f(r_{ik}-r_{ij})/\beta}\cdot e^{-i\pi f(_g t_k - _g t_j)} \tag{3.3}$$

$$F_{ij}(f) = \int_{-\infty}^{\infty} x_{ij}(t)\cdot e^{i2\pi ft}dt \tag{3.4}$$

$$x_{ik}(t) = \int_{-\infty}^{\infty} F_{ik}(f)\cdot e^{i2\pi ft}df \tag{3.5}$$

Figure 3.5 compares the simulated ground motions to the observed ground motions for ISK005 K-NET station (Anamizu). Though the orientations from the epicenter were almost perpendicular between stations, both S wave beginning times and peak accelerations were successfully simulated. Additionally, the phase characteristics of the simulated ground motions harmonized with the observed motions without considering the difference in observed group delay times between two stations, though the phase characteristics between the observed ground motions at two stations are apparently different from each other.

One of next steps of this study shall be an application to a real-time prediction of ground motions using the

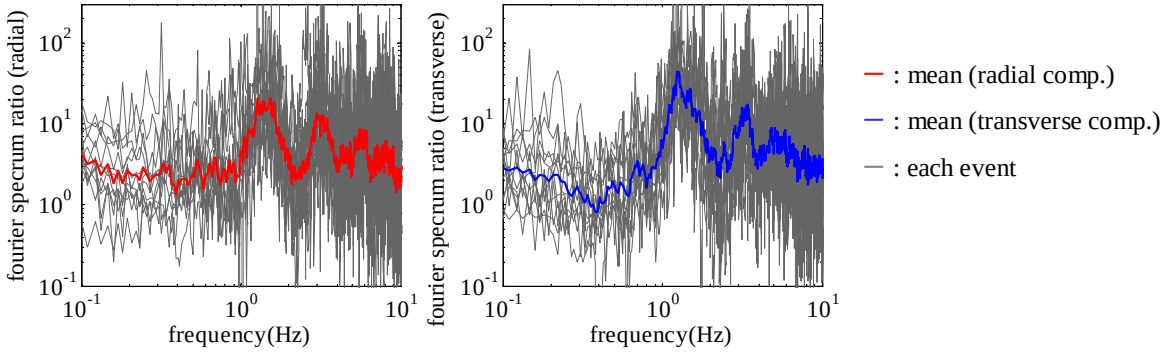

Figure 3.4 Amplitude of Fourier spectrum ratio from ISKH04 (borehole) to ISK005

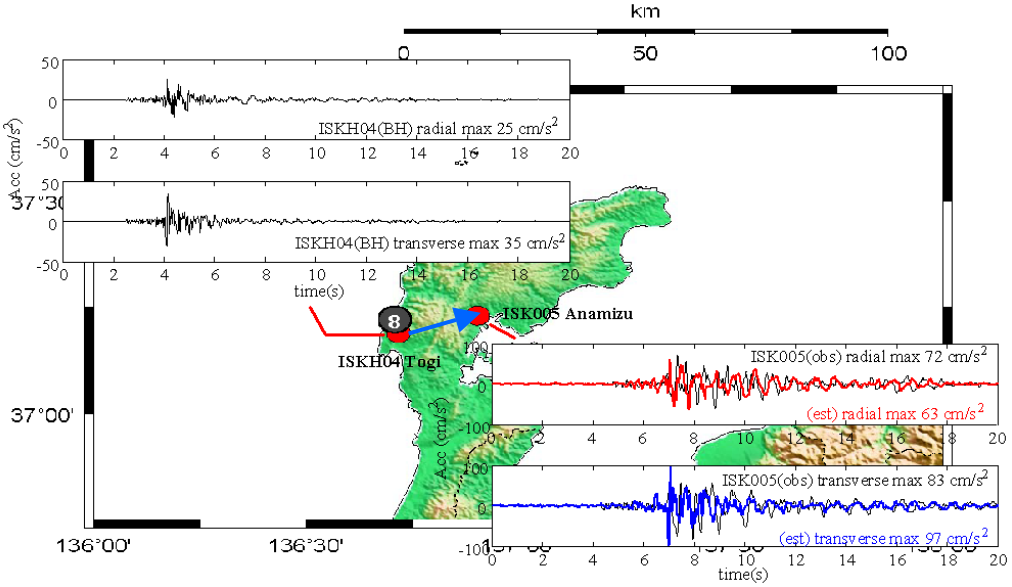

Figure 3.5 Comparison between observed records and simulation results (<10Hz) for M_J 4.6 earthquake at 8:08 Mar 28 2008 (No. 8)

Earthquake Early Warning provided by Japan Meteorological Agency (2007) (Nagashima et al., 2008). Then, an additional difficulty will arise, e.g., in dealing with the size of a fault plane for large earthquakes, which will be discussed in future.

4. CONCLUSIONS

An inversion method was applied to crustal earthquakes in Japan. Qs value for propagation path was evaluated from spectral amplitudes. The scattering due to propagation path was evaluated from an inversion of group delay times. An envelope model considering the scattering was proposed for stochastic Green's function on rock sites. A transfer function from source to site was modeled using stochastic group delay times based on the results of an inversion analysis. Ground motion simulation was also conducted considering local site effects using transfer function between neighboring stations.

REFERENCES

Andrews, D. J. (1981). Separation of Source and Propagation Spectra of Seven Mammoth Lake Aftershocks, *Proceedings of the USGS-NRC Workshop on Strong Motion, Lake Tahoe*.
Birgoren, G. and Irikura, K. (2005). Estimation of Site Response in Time Domain Using the Meyer-Yamada Wavelet Analysis, *Bulletin of Seismological Society of America*, **95:4**, 1447-1456.
Boore, D. M. (1983). Stochastic Simulation of High-Frequency Ground Motions Based on Seismological Models of Radiated Spectra, *Bulletin of Seismological Society of America*, **73:6**, 1865-1894.
Iwata, T. and Irikura, K. (1986). Separation of Source, Propagation and Site Effects from Observed S-Waves, *ZISIN Journal of the Seismological Society of Japan, Second Series*, **39**, 579-593. (in Japanese)
Japan Meteorological Agency. (2007). http://www.jma.go.jp/jma/en/Activities/eew.html.
Kagawa, T. (2004). Developing a Stochastic Green's Function Method having more accuracy in long period range to be used in the Hybrid Method, *Journal of JAEE* **4:2**, 21-32. (in Japanese)
Kamae, K., Irikura, K. and Fukuchi, Y. (1991). Prediction of Strong Ground Motion Based on Scaling Law of Earthquake, *Journal of Structural Construction Engineering* (*Transaction of AIJ*) **430**, 1-9. (in Japanese)
Nagashima, I. Yoshimura, C., Uchiyama, Y., Maseki, R. Itoi, T. (2008). Real-Time Prediction of Earthquake Ground Motion Using Empirical Transfer Function, *The 14th World Conference on Earthquake Engineering*. (in press)
Onishi, Y. and Horike, M. (2000). Application of the method for generating 3-component strong ground motions using the stochastic Green's function to the 1995 Hyogo-ken Nanbu earthquake, *Journal of Structural Engineering* **46B**, 389-398. (in Japanese)
Sato, T. (2004). Study on Envelope Model of Ground Motions Based on Inversion of Group Delay Time and Scattering Theory, *Journal of Structural Construction Engineering* (*Transaction of AIJ*) **586**, 71-78. (in Japanese)
Sato, T. (2006). Path Model for Strong Motion Prediction, *The 34th Symposium of Earthquake Ground Motion, Research Subcommittees on the Earthquake Ground Motion, The Architectural Institute of Japan*, 23-34. (in Jaopanese)
Sawada, S., Morikawa, H. Toki, K. and Yokoyama, K. (1998). Identification of Path and Local Site Effects on Phase Spectrum of Seismic Motion, *Proceedings of the 10th Japan Earthquake Engineering Symposium*, 915-920. (in Japanese)

ACKNOWLEDGEMENTS

We used ground motion records of K-NET and KiK-net by NIED. GMT by Wessel and Smith was used to make several figures. This research was partially supported by JSPS KAKENHI (C) (No. 19510186).